2. Survey of Helical Antennas

2.1 Introduction

The helical antenna is a hybrid of two simple radiating elements, the dipole and loop antennas. A helix becomes a linear antenna when its diameter approaches zero or pitch angle goes to $90°$. On the other hand, a helix of fixed diameter can be seen as a loop antenna when the spacing between the turns vanishes $(\boldsymbol{a} = 0°)$.

Helical antennas have been widely used as simple and practical radiators over the last five decades due to their remarkable and unique properties. The rigorous analysis of a helix is extremely complicated. Therefore, radiation properties of the helix, such as gain, far-field pattern, axial ratio, and input impedance have been investigated using experimental methods, approximate analytical techniques, and numerical analyses. Basic radiation properties of helical antennas are reviewed in this chapter.

The geometry of a conventional helix is shown in Figure 2.1a. The parameters that describe a helix are summarized below.

D = diameter of helix

S = spacing between turns

N = number of turns

C = circumference of helix = $\boldsymbol{p}D$

A = total axial length = NS

$\boldsymbol{a}$ = pitch angle

If one turn of the helix is unrolled, as shown in Figure 2.1(b), the relationships between S, C, a and the length of wire per turn, L, are obtained as:

$$S = L \sin a = C \tan a$$
$$L = (S^2 + C^2)^{1/2} = (S^2 + p^2 D^2)^{1/2}$$

2.2 Modes of Operation

2.2.1 Transmission Modes

An infinitely long helix may be modeled as a transmission line or waveguide supporting a finite number of modes. If the length of one turn of the helix is small compared to the wavelength, $L \ll l$, the lowest transmission mode, called the T_0 mode, occurs. Figure 2.2a shows the charge distribution for this mode.

When the helix circumference, C, is of the order of about one wavelength $(C \approx 1l)$, the second-order transmission mode, referred to as the T_1 mode, occurs. The charge distribution associated with the T_1 mode can be seen in Figure 2.2b. Higher-order modes can be obtained by increasing of the ratio of circumference to wavelength and varying the pitch angle.

2.2.2 Radiation Modes

When the helix is limited in length, it radiates and can be used as an antenna. There are two radiation modes of important practical applications, the normal mode and the axial mode. Important properties of normal-mode and axial-mode helixes are summarized below.
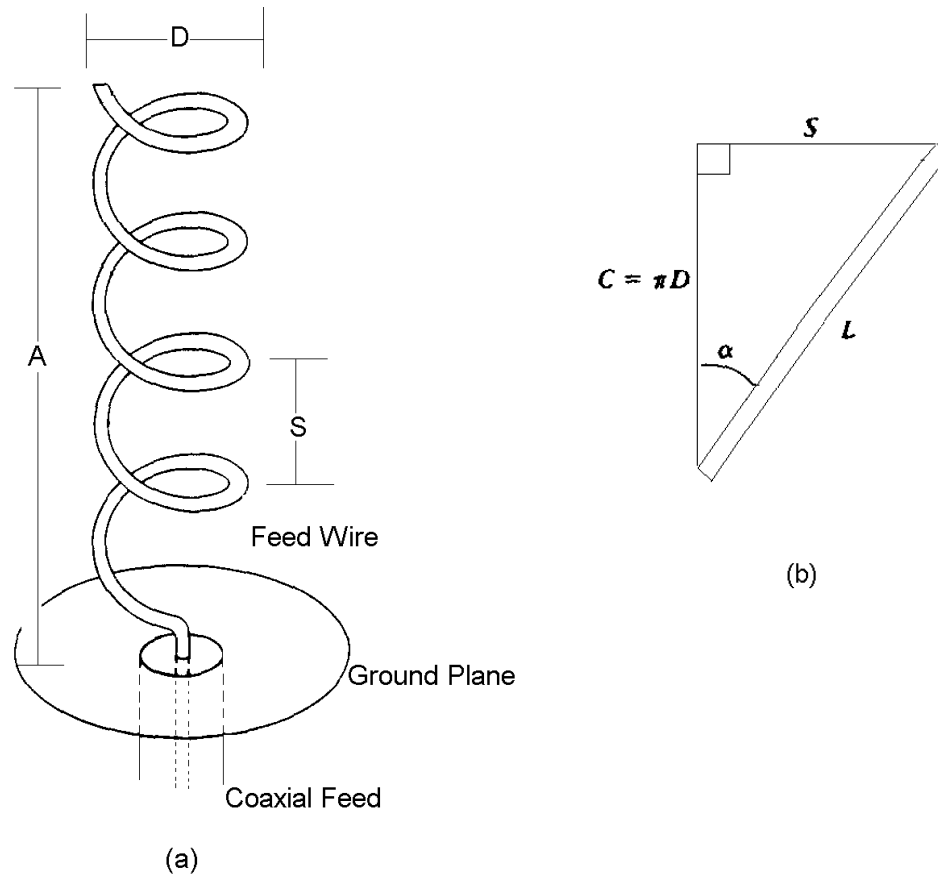
Figure 2.1   **(a) Geometry of helical antenna; (b) Unrolled turn of helical antenna**
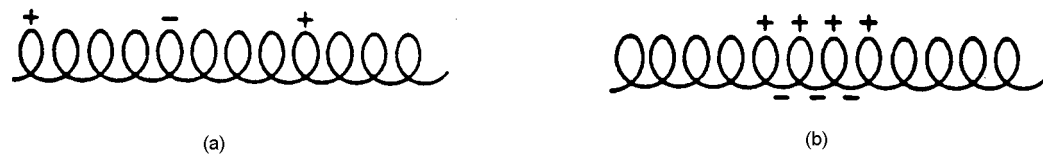

Figure 2.2   **Instantaneous charge distribution for transmission modes: (a) The lowest-order mode (T_0); (b) The second-order mode (T_1)**

2.2.2.1 Normal Mode

For a helical antenna with dimensions much smaller than wavelength $(NL << l)$, the current may be assumed to be of uniform magnitude and with a constant phase along the helix [5]. The maximum radiation occurs in the plane perpendicular to the helix axis, as shown in Figure 2.3a. This mode of operation is referred to as the "normal mode". In general, the radiation field of this mode is elliptically polarized in all directions. But, under particular conditions, the radiation field can be circularly polarized. Because of its small size compared to the wavelength, the normal-mode helix has low efficiency and narrow bandwidth.

2.2.2.2 Axial Mode

When the circumference of a helix is of the order of one wavelength, it radiates with the maximum power density in the direction of its axis, as seen in Figure 2.3b. This radiation mode is referred to as "axial mode". The radiation field of this mode is nearly circularly polarized about the axis. The sense of polarization is related to the sense of the helix winding.

In addition to circular polarization, this mode is found to operate over a wide range of frequencies. When the circumference (C) and pitch angle (a) are in the ranges of $\frac{3}{4} < \frac{C}{l} < \frac{4}{3}$ and $12° < a < 15°$ [6], the radiation characteristics of the axial-mode helix remain relatively constant. As stated in [7] ,"if the impedance and the pattern of an antenna do not change significantly over about one octave ($\frac{f_u}{f_l} = 2$) or more, we will classify it as a broadband antenna". It is noted that the ratio of the upper frequency to the lower frequency of the axial-mode helix is equal to $\frac{f_u}{f_l} = \frac{4/3}{3/4} = 1.78$. This is close to the definition of broadband antennas. For the reason that the axial-mode helix possesses a
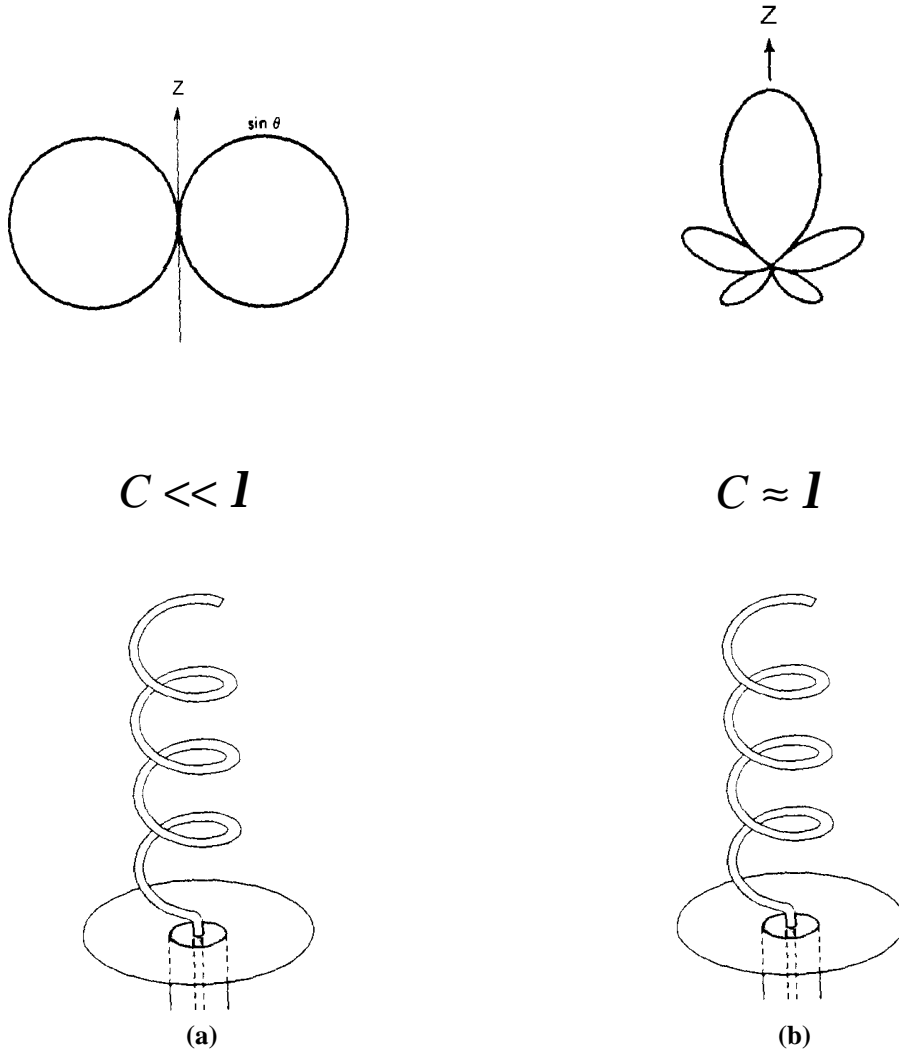
$$C << 1 \qquad\qquad C \approx 1$$

Figure 2.3   **Radiation patterns of helix: (a) Normal mode; (b) Axial mode**

number of interesting properties, including wide bandwidth and circularly polarized radiation, it has found many important applilcations in communication systems.

2.3 Analysis of Helix

Unlike the dipole and loop antennas, the helix has a complicated geometry. There are no exact solutions that describe the behavior of a helix. However, using experimental methods and approximate analytical or numerical techniques, it is possible to study the radiation properties of this antenna with sufficient accuracy. This section briefly discusses the analysis of normal-mode and axial-mode helices.

2.3.1 Normal-Mode Helix

The analysis of a normal-mode helix is based on a uniform current distribution over the length of the helix.   Furthermore, the helix may be modeled as a series of small loop and short dipole antennas as shown in Figure 2.4. The length of the short dipole is the same as the spacing between turns of the helix, while the diameter of the loop is the same as the helix diameter.

Since the helix dimensions are much smaller than wavelength, the far-field pattern is independent of the number of turns. It is possible to calculate the total far-field of the normal-mode helix by combining the fields of a small loop and a short dipole connected in series. Doing so, the result for the electric field is expressed as [6]

$$\vec{E} = j\boldsymbol{h}\frac{kI_0e^{-jkr}}{4\boldsymbol{p}r}\sin\boldsymbol{q}(S\hat{\boldsymbol{q}} - j\frac{\boldsymbol{p}^2D^2}{2\boldsymbol{l}}\hat{\boldsymbol{f}}), \qquad (2.1)$$

where $k = \dfrac{2p}{l}$ is the propagation constant, $h = \sqrt{\dfrac{m}{e}}$ is the intrinsic impedance of the medium, and I_0 is a current amplitude. As noted in (2.1), the q and f components of the field are in phase quadrature. Generally, the polarization of this mode is elliptical with an axial ratio given by

$$AR = \frac{|E_q|}{|E_f|} = \frac{2Sl}{p^2 D^2} .$$
(2.2)

The normal-mode helix will be circularly polarized if the condition $AR = 1$ is satisfied. As seen from (2.2), this condition is satisfied if the diameter of the helix and the spacing between the turns are related as

$$C = \sqrt{2Sl} .$$
(2.3)

It is noted that the polarization of this mode is the same in all directions except along the z-axis where the field is zero. It is also seen from (2.1) that the maximum radiation occurs at $q = 90°$; that is, in a plane normal to the helix axis.

2.3.2 Axial-Mode Helix

Unlike the case of a normal-mode helix, simple analytical solutions for the axial-mode helix do not exist. Thus, radiation properties and current distributions are obtained using experimental and approximate analytical or numerical methods.

The current distribution of a typical axial-mode helix is shown in Figure 2.5 [5]. As noted, the current distribution can be divided into two regions. Near the feed region, the current attenuates smoothly to a minimum, while the current amplitude over the remaining length of the helix is relatively uniform. Since the near-feed region is small compared to the length of the helix, the current can be approximated as a travelling wave of constant amplitude. Using this approximation, the far-field pattern of the axial-mode helix can be analytically determined. There are two methods for the analysis of far-field pattern. In the first method, an N-turn helix is considered as an array of N elements with

an element spacing equal to S. The total field pattern is then obtained by multiplying the pattern of one turn of the helix by the array factor. The result is

$$F(\boldsymbol{q}) = c_0 \cos\boldsymbol{q}\, \frac{\sin(N\boldsymbol{y}/2)}{\sin(\boldsymbol{y}/2)}, \tag{2.4}$$

where c_0 is a constant coefficient and $\boldsymbol{y} = kS\cos\boldsymbol{q} + \boldsymbol{a}$. Here, $\boldsymbol{a}$ is the phase shift between successive elements and is given as

$$\boldsymbol{a} = -2\boldsymbol{p} - \frac{\boldsymbol{p}}{N}. \tag{2.5}$$

In (2.4), $\cos\boldsymbol{q}$ is the element pattern and $\dfrac{\sin(N\boldsymbol{y}/2)}{\sin(\boldsymbol{y}/2)}$ is the array factor for a uniform array of N equally-spaced elements. As noted from (2.5), the Hansen-Woodyard condition is satisfied. This condition is necessary in order to achieve agreement between the measured and calculated patterns.

In a second method, the total field is directly calculated by integrating the contributions of the current elements from one end of the helix to another. The current is assumed to be a travelling wave of constant amplitude. The current distribution at an arbitrary point on the helix is written as [6]

$$\bar{\mathrm{I}}(l) = \mathrm{I}_0 \exp(-jg\boldsymbol{f}')\hat{\mathrm{I}}, \tag{2.6}$$

where

$\qquad\qquad l =$ the length of wire from the beginning of the helix to an

$\qquad\qquad\qquad$ arbitrary point

$$g = \frac{\boldsymbol{w}L_T}{pc\boldsymbol{f}'_m}$$

$\qquad\qquad L_T =$ the total length of the helix

$\qquad\qquad p =$ phase velocity of wave propagation along the helix

$\qquad\qquad\qquad$ relative to the velocity of light, c
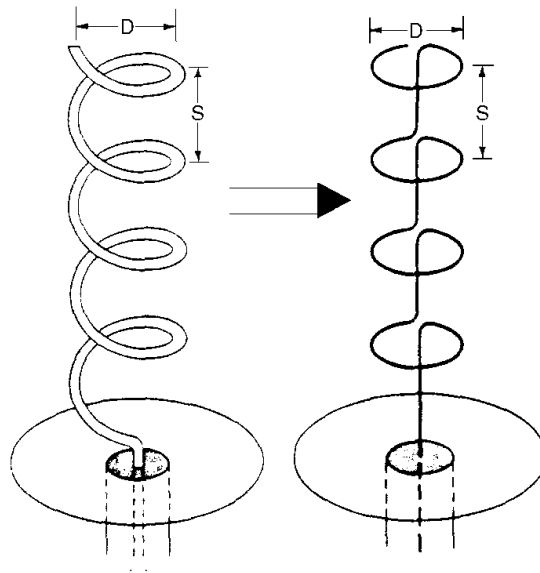
Figure 2.4   Approximating the geometry of normal-mode helix
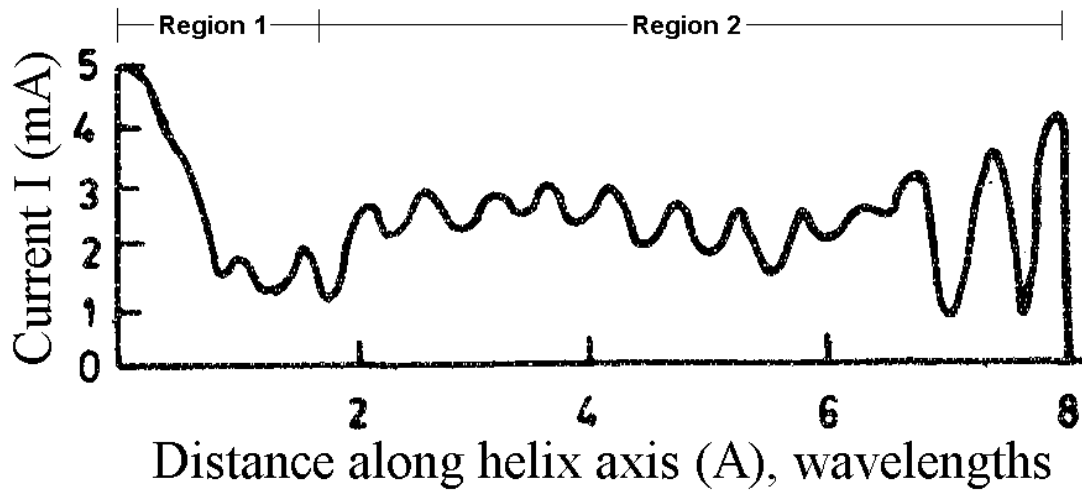
Figure 2.5   Measured current distribution on axial-mode helix [5]

$$= \frac{1}{\sin \boldsymbol{a} + \left[(2N+1) \big/ N \right] (l \cos \boldsymbol{a}) \big/ C}$$ (according

to Hansen-Woodyard condition)

$$= 2\boldsymbol{p}N$$

$\boldsymbol{f}' =$ azimuthal coordinate of an arbitrary point

$\hat{\mathrm{I}} =$ unit vector along the wire

$= -\hat{x} \sin \boldsymbol{f}' + \hat{y} \cos \boldsymbol{f}' + \hat{z} \sin \boldsymbol{a}$

The magnetic vector potential at an arbitrary point in space is obtained as [6]

$$\vec{\mathrm{A}}(\vec{r}) = \frac{\boldsymbol{m}_0 \mathrm{I}_0 \exp(-jkr)}{4\boldsymbol{p}r} \int_0^{f_m} \exp[\, ju \cos(\boldsymbol{f} - \boldsymbol{f}')] \exp(\, jd\boldsymbol{f}') \hat{\mathrm{I}} d\boldsymbol{f}' , (2.7)$$

Where
$u = ka \sin \boldsymbol{q}$

$a = $ radius of the helix

$d = B - g$

$B = ka \cos \boldsymbol{q} \tan \boldsymbol{a}$

Finally, the far-field components of the electric field, E_q and E_f, can be expressed as

$$E_q = -j\boldsymbol{w}[(A_x \cos \boldsymbol{f} + A_y \sin \boldsymbol{f}) \cos \boldsymbol{q} + A_z \sin \boldsymbol{q}] , \qquad (2.8)$$

$$E_f = -j\boldsymbol{w}(A_y \cos \boldsymbol{f} - A_x \sin \boldsymbol{f}) . \qquad (2.9)$$

2.3.3 Empirical Relations for Radiation Properties of Axial-Mode Helix

Approximate expressions for radiation properties of an axial-mode helix have also been obtained empirically. A summary of the empirical formulas for radiation characteristics is presented below. These formulas are valid when $12° < \boldsymbol{a} < 15°$, $\frac{3}{4} < C_l < \frac{4}{3}$ and $N > 3$.

An approximate directivity expression is given as [1]

$$D \approx C_I{}^2 NS \; , \tag{2.10}$$

C_I and S_I are, respectively, the circumference and spacing between turns of the helix normalized to the free space wavelength (λ). Since the axial-mode helix is nearly lossless, the directivity and the gain expressions are approximately the same.

In 1980, King and Wong [8] reported that Kraus's gain formula (2.10) overestimates the actual gain and proposed a new gain expression using a much larger experimental data base. The new expression is given as

$$G_P = 8.3 \left(\frac{pD}{\lambda_P} \right)^{\sqrt{N+2}-1} \left(\frac{NS}{\lambda_P} \right)^{0.8} \left[\frac{\tan 12.5^\circ}{\tan a} \right]^{\sqrt{N}/2} , \tag{2.11}$$

where λ_P is the free-space wavelength at peak gain.

In 1995, Emerson [9] proposed a simple empirical expression for the maximum gain based on numerical modeling of the helix. This expression gives the maximum gain in dB as a function of length normalized to wavelength ($\bar{L}_T = L_T / \lambda$).

$$G_{max} (\text{dB}) = 10.25 + 1.22\bar{L}_T - 0.0726\bar{L}_T{}^2 . \tag{2.12}$$

Equation (2.12), when compared with the results from experimental and theoretical analyses, gives the gain reasonably accurately.

Half-Power Beamwidth

The empirical formula for the half-power beamwidth is [1]

$$HPBW = \frac{52}{C_I \sqrt{NS_I}} \quad (\text{degrees}). \tag{2.13}$$

A more accurate formula was later presented by King and Wong using a larger experimental data base [10]. This result is

$$HPBW = \frac{61.5 \left(\dfrac{2N}{N+5} \right)^{0.6}}{\left(\dfrac{pD}{l} \right)^{\sqrt{N}/4} \left(\dfrac{NS}{l} \right)^{0.7}} \left(\frac{\tan a}{\tan 12.5°} \right)^{\sqrt{N}/4} \quad \text{(degrees).} \qquad (2.14)$$

Input Impedance

Since the current distribution on the axial-mode helix is assumed to be a travelling wave of constant amplitude (Section 2.3.2), its terminal impedance is nearly purely resistive and is constant with frequency. The empirical formula for the input impedance is

$$R = 140 C_l \qquad \text{(ohms).} \qquad (2.15)$$

The input impedance, however, is sensitive to feed geometry. Our numerical modeling of the helix indicated that (2.15) is at best a crude approximation of the input impedance.

Bandwidth

Based on the work of King and Wong [8], an empirical expression for gain bandwidth, as a frequency ratio, has been developed:

$$\frac{f_U}{f_L} \approx 1.07 \left(\frac{0.91}{G/G_P} \right)^{4/(3\sqrt{N})}, \qquad (2.16)$$

where f_U and f_L are the upper and lower frequencies, respectively, G_P is the peak gain from equation (2.11), and G is the gain drop with respect to the peak gain.

2.3.4 Optimum Performance of Helix

Many different configurations of the helix have been examined in search of an optimum performance entailing largest gain, widest bandwidth, and/or an axial ratio closest to unity. The helix parameters that result in an optimum performance are

summarized in Table 2.1. There are some helices with parameters outside the ranges in Table 2.1 that exhibit unique properties. However, such designs are not regarded as optimum, because not all radiation characteristics meet desired specifications. A summary of the effects of various parameters on the performance of helix is presented below [2].

Table 2.1 Parameter ranges for optimum performance of helix

Parameter	Optimum Range
Circumference	$\frac{3}{4}l < C < \frac{4}{3}l$
Pitch angle	$11° < a < 14°$
Number of turns	$3 < N < 15$
Wire diameter	Negligible effect
Ground plane diameter	At least $\frac{1}{2}l$

Circumference

As shown in Figure 2.6, it is noted that the optimum circumference for achieving the peak gain is around $1.1l$ and is relatively independent of the length of the helix. Other results show that the peak gain smoothly drops as the diameter of the helix decreases (Figure 2.7). Since other parameters of the helix also affect its properties, a circumference of $1.1l$ is viewed as a good estimate for an optimum performance.

Pitch Angle

Keeping the circumference and the length of a helix fixed, the gain increases smoothly when the pitch angle is reduced, as seen in Figure 2.8. However, the reduction
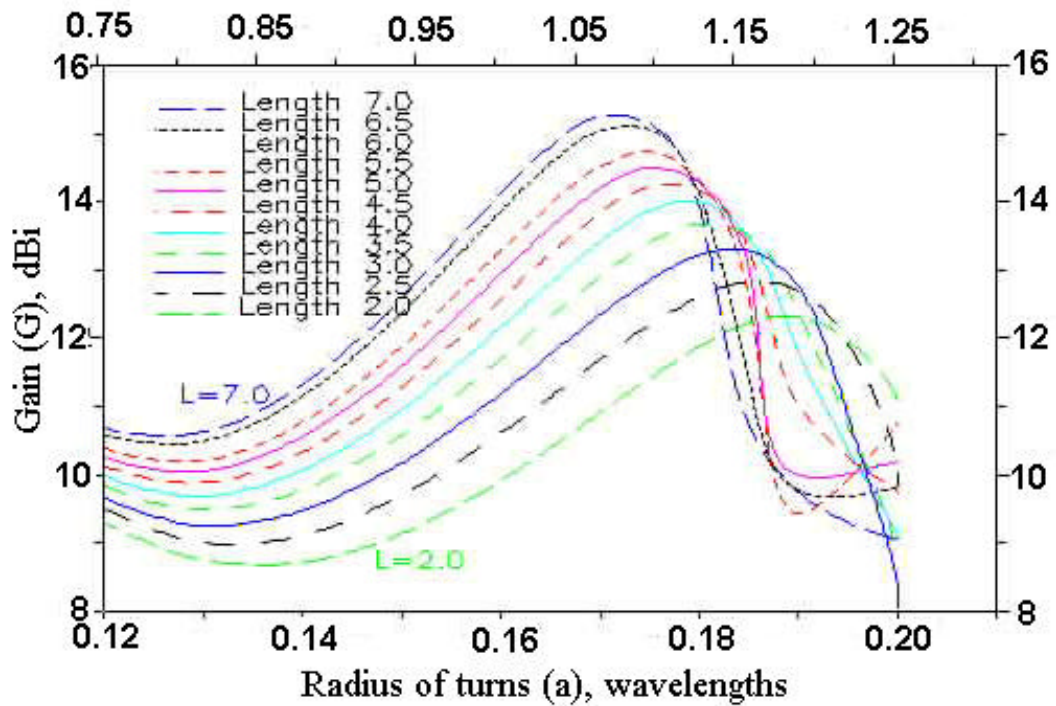
Figure 2.6 Gain of helix for different lengths as function of normalized circumference (C_1) [9]
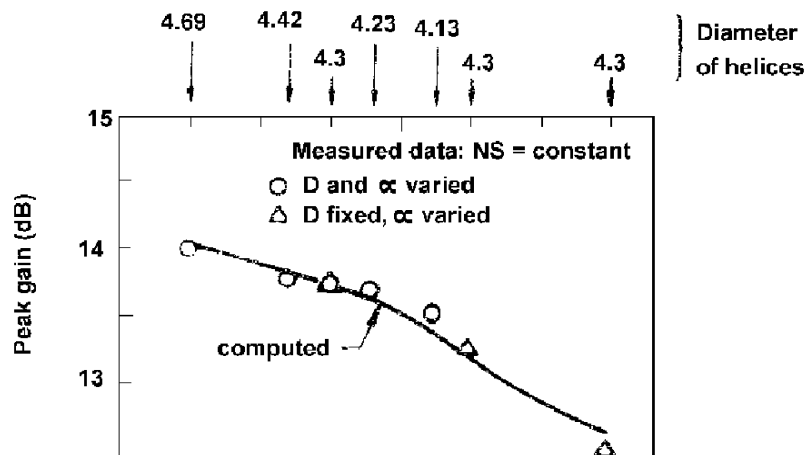

Figure 2.7 Peak gain of various diameter as D and a varied (circles), D fixed and a varied (triangle) [8].

of pitch angle is limited by the bandwidth performance. That is, a narrower bandwidth is obtained for a helix with a smaller pitch angle. For this reason, it has been generally agreed that the optimal pitch angle for the axial-mode helix is about $12.5°$.

Number of Turns

Many properties, such as gain, axial ratio, and beamwidth, are affected by the number of turns. Figure 2.9 shows the variation of gain versus the number of turns. It is noted that as the number of turns increases, the gain increases too. The increase in gain is simply explained using the uniformly excited equally-spaced array theory. However, the gain does not increase linearly with the number of turns, and, for very large number of turns, adding more turns has little effect. Also, as shown in Figure 2.10, the beamwidth becomes narrower for larger number of turns. Although adding more turns improves the gain, it makes the helix larger, heavier, and more costly. Practical helices have between 6 and 16 turns. If high gain is required, array of helices may be used.

Conductor Diameter

This parameter does not significantly affect the radiation properties of the helix. For larger conductor diameters, slightly wider bandwidths are obtained. Also, thicker conductors can be used for supporting a longer antenna.

Ground Plain

The effect of ground plain on radiation characteristics of the helix is negligible since the backward traveling waves incident upon it are very weak [7]. Nevertheless, a ground plane with a diameter of one-half wavelength at the lowest frequency is usually recommended.
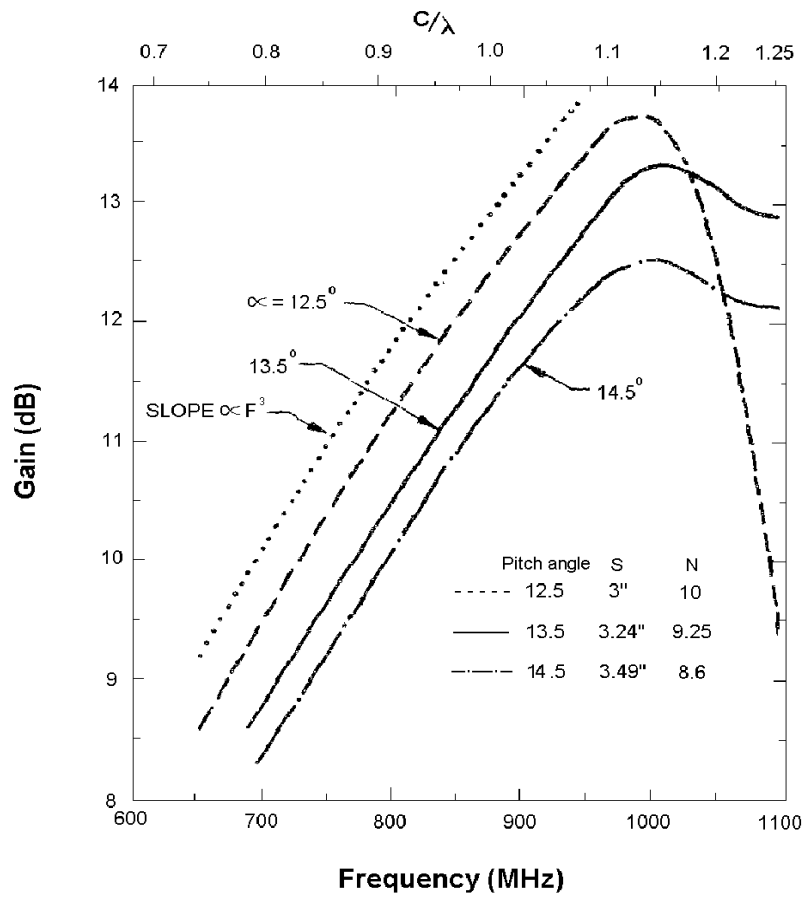
Figure 2.8 **Gain versus frequency of 30.8-inch length and 4.3-inch diameter helix for different pitch angles [8].**
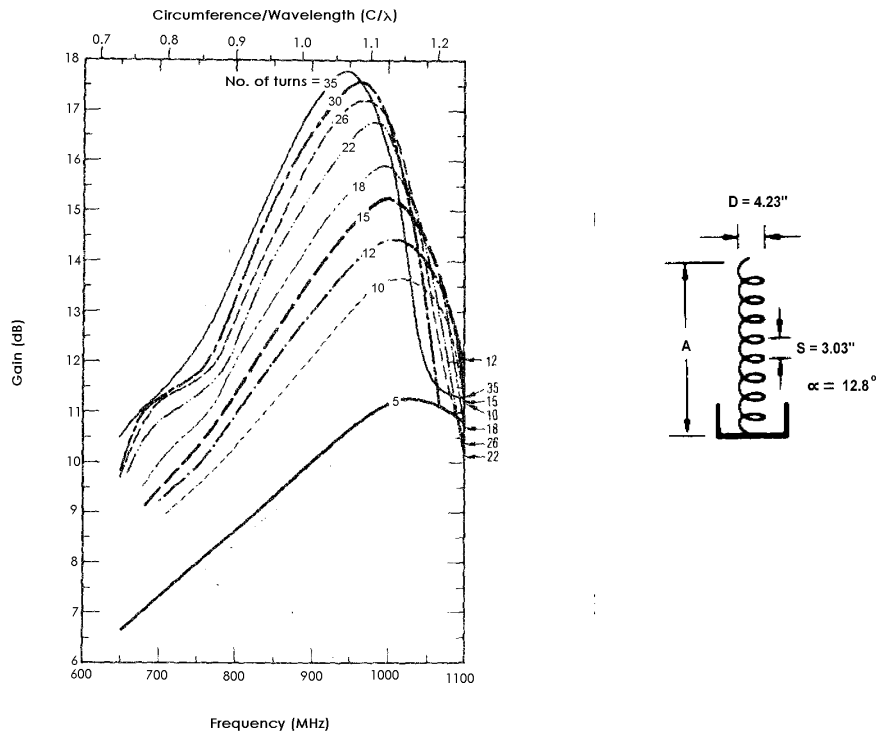
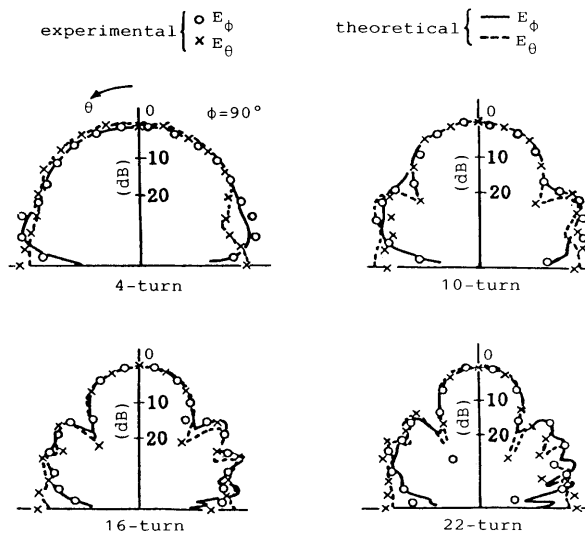**Figure 2.9**   **Gain versus frequency for 5 to 35-turn helical antennas with 4.23-inch diameter [8]**

Figure 2.10   **Radiation patterns for various helical turns of helices with $a = 12°$ and $C = 10cm.$ at 3 GHz [12].**

2.4 Modified Helices

Various modifications of the conventional helical antenna have been proposed for the purpose of improving its radiation characteristics. A summary of these modifications is presented below.

2.4.1 Helical Antenna with Tapered End

Nakano and Yamauchi [11] have proposed a modified helix in which the open end section is tapered as illustrated in Figure 2.11. This structure provides significant improvement in the axial ratio over a wide bandwidth. According to them, the axial ratio improves as the cone angle q_t is increased. For a helix with pitch angle of $12.5°$ and 6 turns followed by few tapered turns, they obtained an axial ratio of 1:1.3 over a frequency range of 2.6 to 3.5 GHz.

2.4.2 Printed Resonant Quadrifilar Helix

Printed resonant quadrifilar helix is a modified form of the resonant quadrifilar helix antenna first proposed by Kilgus [13]. The structure of this helix consists of 4 microstrips printed spirally around a cylindrical surface. The feed end is connected to the opposite radial strips as seen in Figure 2.12. The advantage of this antenna is a broad beam radiation pattern (half-power beamwidth $> 145°$). Additionally, its compact size and light weight are attractive to many applications especially for GPS systems [14].

2.4.3 Stub-Loaded Helix

To reduce the size of a helix operating in the axial mode, a novel geometry referred to as stub-loaded helix has been recently proposed [15]. Each turn contains four stubs as illustrated in Figure 2.13. The stub-loaded helix provides comparable radiation

properties to the conventional helix with the same number of turns, while offering an approximately 4:1 reduction in the physical size.

2.4.4 Monopole-Helix Antenna

This antenna consists of a helix and a monopole, as shown in Figure 2.14, [16]. The purpose of this modified antenna is to maintain operation at two different frequencies, applicable to dual-band cellular phone systems operating in two different frequency bands (900 MHz for GSM and 1800 MHz for DCS1800).
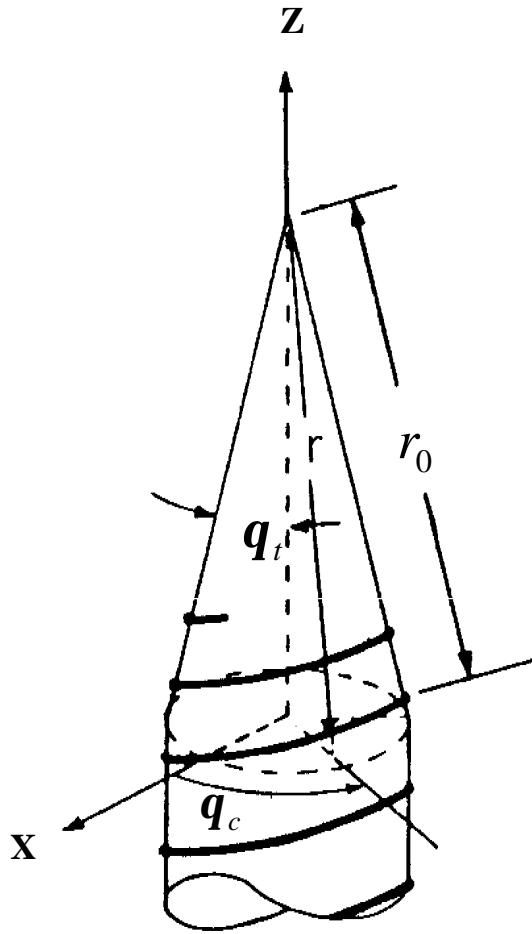
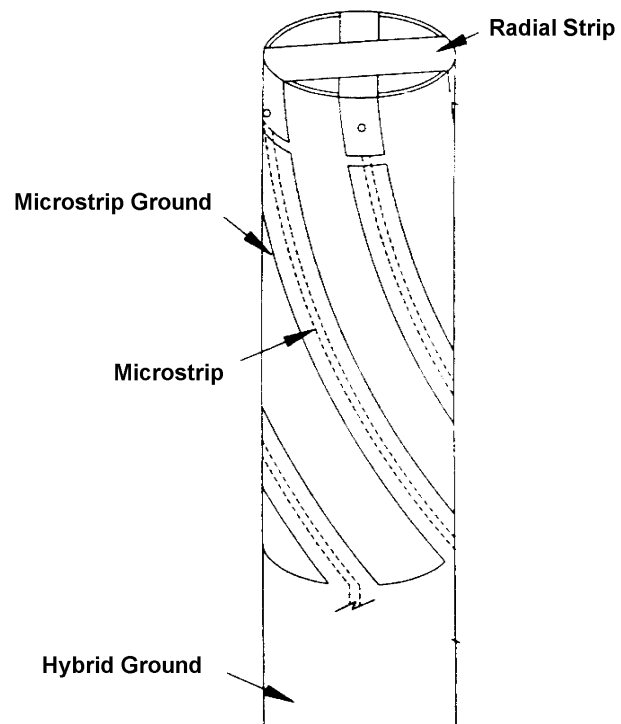**Figure 2.11 Tapered helical antenna configuration.[11].**

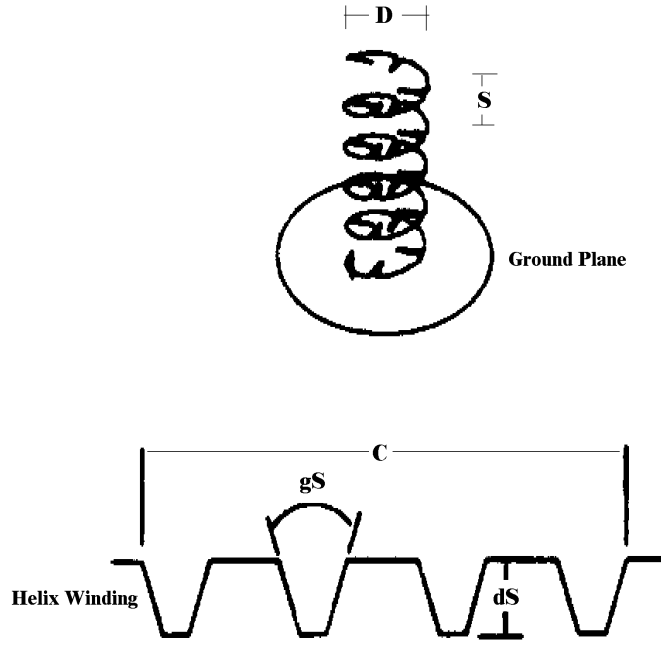**Figure 2.12** $\frac{1}{2}$ turn half-wavelength printed resonant quadrifilar helix [14].
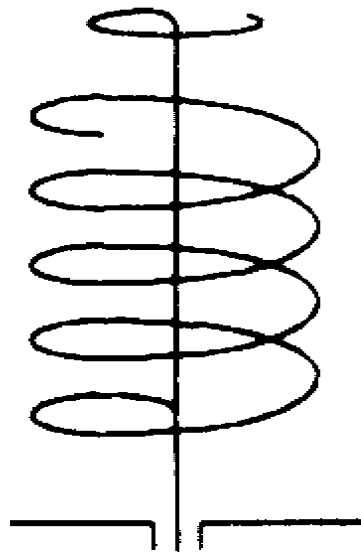
Figure 2.13 Stub-loaded helix configuration [15].

Figure 2.14 Monopole-helix antenna [16].